Article

Not peer-reviewed version

A Ratiometric Fluorescence Detection Method for Berberine Using Triplex-Containing DNA-Templated Silver Nanoclusters

Ming Zhu , Mingyang Sun , Juntong Liu , Changbao Chen , Yonggang Yang * , Ye Teng *

Posted Date: 17 June 2024

doi: 10.20944/preprints202406.1050.v1

Keywords: berberine; DNA-AgNCs; triplex; ratiometric fluorescence

 doi:10.20944/preprints202406.1050.v1

Article

A Ratiometric Fluorescence Detection Method for Berberine Using Triplex-Containing DNA-Templated Silver Nanoclusters

Ming Zhu, Mingyang Sun, Juntong Liu, Changbao Chen, Yonggang Yang * and Ye Teng *

[1] School of Pharmacy, Changchun University of Chinese Medicine, 1035 Boshuo Road, Changchun, 130117, China

* Correspondence: yangygccucm@163.com; tengye@ccucm.edu.cn

Abstract: Berberine (BBR), as a natural isoquinoline alkaloid, has been demonstrated various pharmacological activities, and widely applied in the treatment of diseases. The quantitative analysis of BBR is important for its pharmacological researches and clinical applications. In the work, utilizing the specific interaction between BBR and triplex DNA, a sensitive and selective fluorescent detecting method was established with DNA-templated silver nanoclusters (DNA-AgNCs). After binding with the triplex structure in the template of DNA-AgNCs, BBR quenched the fluorescence of DNA-AgNCs and formed BBR-triplex complex with yellow-green fluorescence. The ratiometric fluorescence signal showed a linear relationship with BBR concentration in a range between 10 nM to 1000 nM, with a detect limit of 10 nM. Our method exhibited excellent sensitivity and selectivity, and it was further applied in BBR detection in real samples.

Keywords: berberine; DNA-AgNCs; triplex; ratiometric fluorescence

1. Introduction

BBR is a natural isoquinoline alkaloid, which is considered as the major effective content of many Chinese medical herbs such as *Coptis chinensis* and *Phellodendron amurense* [1]. It has been widely used in pharmacological researches and disease treatment due to its multiple pharmacological activities, including anti-inflammatory, antimicrobial, anticancer activities and so on [2]. For example, the new synthesis methods and structural modification of BBR and its derivatives have been attempted to improve the bioavailability and to clarify the anti-inflammatory pathway and anti-inflammatory structure-activity relationships [3,4]. Researchers also found that the mechanism of BBR in lipid-lowering and insulin resistance might be related to its impact on the gastrointestinal microbiota [5]. Moreover, BBR was reported to significantly inhibit the migration and invasion of cancer cells by down-regulating the expression of specific genes or pathways [6].

Interestingly, BBR was demonstrated to have good binding affinity with specific structures of DNA/RNA such as duplex [7,8], triplex [8,9], G-quadruplex [10], and i-motif [11], which expanded its applications in biological fields. For example, BBR was considered as a promising G-quadruplex stabilizer which might suppress cancer and viral gene expression [10]. Xu et al. developed label-free DNA-based logic gates utilizing the specific interaction between BBR and i-motif [11].

The multiple functions and clinical effects made quantitative analysis of BBR important for its mechanism study. Various analytical methods for BBR quantification have been established, including colorimetric assay [12], chemiluminescence [13], fluorescence [14,15], electrochemical analysis [16], high-performance liquid chromatography (HPLC) [17], mass spectrometry [18], resonance light scattering technique (RLS) [19], etc. However, many of these detection methods are suffered from complicated sample pretreatment, complex operation, expensive instrument, time-consuming process, poor sensitivity or selectivity. Notably, detecting methods with excellent fluorescent probes are favorable in BBR quantification because of the stable fluorescence signal,

 doi:10.20944/preprints202406.1050.v1

simple sample preparation, fast detection speed, high sensitivity and low cost. The well-designed novel fluorescent probes are desired.

Metal nanoclusters, such as silver nanoclusters (AgNCs) and gold nanoclusters (AuNCs), are a class of fluorescent probes with nanoscale and strong fluorescence, which have been widely applied in the detection of biomolecules and cell imaging [20,21]. Among them, AgNCs is characterized by its excellent photophysical properties, low cost, good biocompatibility and low toxicity [22]. Especially, DNA-AgNCs have attracted researchers interests because of their excellent fluorescence properties and alterable excitation/emission wavelengths [23]. The specific binding between DNA sequences and biomolecules could greatly improve the selectivity of detecting methods based on DNA-AgNCs. Therefore, various DNA-AgNCs probes have been designed and applied in the detection of DNAs/RNAs, metal ions, enzymes, proteins, and other active biological molecules [24,25].

Herein, a novel fluorescent probe of DNA-AgNCs was designed for BBR detection utilizing the intercalative binding of BBR and DNA triplex structure. A hairpin structure with C6-loop was used for fluorescent DNA-AgNCs synthesis. The stem could form triplex in the presence of a single complementary strand, providing intercalative binding sites for BBR. The formation of BBR-triplex complex significantly quenched the fluorescence of DNA-AgNCs and an increasing emission of BBR-triplex complex was found. The ratiometric fluorescence signal was correlated to BBR concentration in a range between 10 nM to 1000 nM. A sensetive and selective detecting method was achieved with a detection limit of 10 nM. It was further applied in the detection of BBR in real samples and obtained accurate and reliable results.

2. Results

2.1. Characterization of Triplex-Containing DNA-AgNCs

A triplex-containing template was designed for DNA-AgNCs synthesis, which composed of a hairpin structured DNA (Hp-loop1, Table 1) and a short complementary sequence (Hp-ss1, Table 1). Figure 1 showed a schematic diagram of the DNA template structure and the synthesis of DNA-AgNCs. Hp-loop1 contained a C6 loop for the protection of AgNCs and a full-matched stem for triplex formation with Hp-ss1. The DNA-AgNCs were synthesized in a PB buffer at pH 6.0 according to previous reports [26]. The obtained DNA-AgNCs were transparent and colorless, and exhibited red emission under UV light (Figure 2a, inset). Figure 2a showed that the fluorescence excitation and emission spectra of synthesized DNA-AgNCs. A red fluorescence emission at 660 nm was detected when DNA-AgNCs were excited at 590nm. The fluorescence of DNA-AgNCs kept stable in two days, and gradually decreased to about 20% after 10 days (Figure 2b). The sizes of DNA-AgNCs were further characterized by TEM (Figure 2c). Most of synthesized DNA-AgNCs were smaller than 10 nm, and the average diameter of DNA-AgNCs was 3.60 nm.

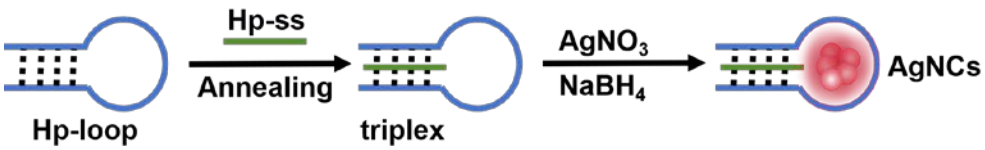

Figure 1. The schematic demonstration of the synthesis of triplex-containing DNA-AgNCs .

Table 1. DNA sequences used in this work.

Name	Sequences(5′-3′)
Hp-loop1	CTTTCTTCCTTCCCCCCAAGGAAGAAAG
Hp-ss1	TTCCTTCTTTC
Hp-loop2	CTTCCTTCCCTCCCCCCAGGGAAGGAAG
Hp-ss2	TCCCTTCCTTC
Hp-loop3	CTTTTTTCTTTCCCCCCAAAGAAAAAAG

 doi:10.20944/preprints202406.1050.v1

Hp-ss3	TTTCTTTTTTC

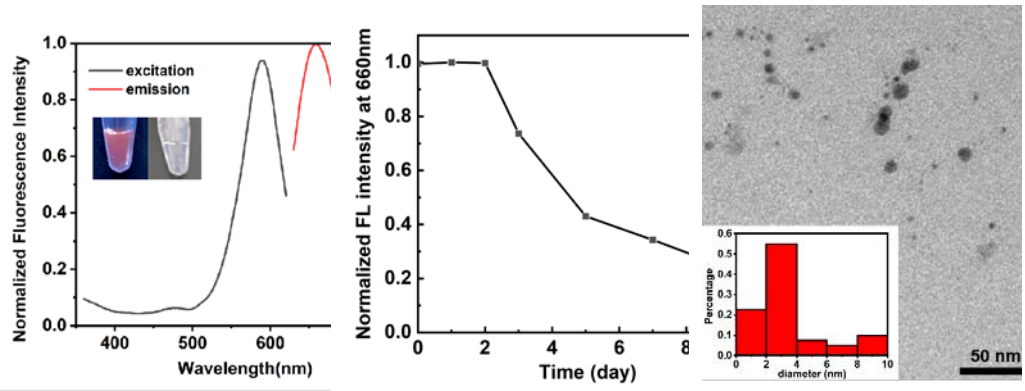

(**a**) (**b**) (**c**)

Figure 2. (**a**) The excitation and emission spectra of DNA-AgNCs (inset: the photos of DNA-AgNCs under UV light and sun light respectively); (**b**) The normalized fluorescence intensity at 660 nm after synthesis for 0, 1, 2, 3, 5, 7 and 10 days. (**c**) The TEM image of DNA-AgNCs (inset: size distribution of DNA-AgNCs).

The structure of template was characterized by CD spectra as shown in Figure S1. Hp-loop1 showed a negative peak at 255 nm, and a positive peak at 275 nm, demonstrated the formation of hairpin structure. In the presence of Hp-ss1, a negative peak at 215 nm existed, suggested the formation of triplex in the stem. Considering the effect of pH on triplex formation, the fluorescence of DNA-AgNCs were compared in PB buffers at pH 6.0, 7.0 and 7.5 respectively (Figure 3b). DNA-AgNCs synthesized in pH 6.0 had better fluorescence intensity, which may be due to the fact that AgNCs preferred to locate in C6 loop rather than triplex formed in the stem under acidic condition.

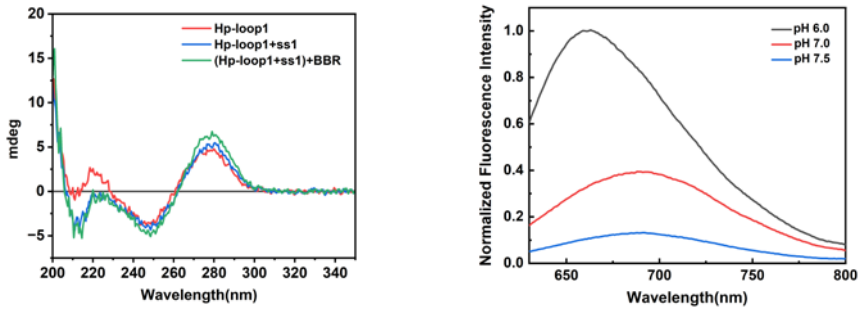

(**a**) (**b**)

Figure 3. (**a**) The CD spectra of Hp-loop1, Hp-loop1+ss1 and Hp-loop1+ss1+BBR; (**b**) The fluorescence emission spectra of (Hp-loop1+ss1)-AgNCs in the buffers at pH 6.0, 7.0 and 7.5.

2.2. The Interaction between DNA-AgNCs and BBR

To verify the potential application of synthesized DNA-AgNCs probes in BBR detection, the interactions between DNA-AgNCs and BBR were investigated. As shown in Figure 3, after the addition of BBR, an obvious color change from red to yellow green was observed under UV light (Figure 4a). The fluorescence of DNA-AgNCs at 660 nm were quenched (Figure 4b), and an emission at 560 nm excited by 360 nm was greatly enhanced (Figure 4c). No fluorescence at 560 nm was detected in the absence of BBR or triplex, suggested that this emission peak was generated from the combination of BBR and triplex. Moreover, triplex-containing DNA-AgNCs showed higher

 doi:10.20944/preprints202406.1050.v1

fluorescence intensity at 560 nm comparing with triplex-containg DNA after interacting with BBR. It might be that the formation of AgNCs in loop region stabilized the triplex formation in stem region spatially. The UV-Vis spectra of DNA-AgNCs in the absence and presence of BBR were corresponding to the fluorescence results (Figure 4d). DNA-AgNCs had an absorption peak at 590 nm which was consistent with their fluorescence excitation wavelength. After the addition of BBR, a new absorption peak appeared at 360 nm, corresponding to the fluorescence spectra of BBR-triplex complex. The absorption peak of DNA-AgNCs had no obvious change, suggested that the quenching of DNA-AgNCs might due to the non-radiative energy transfer.

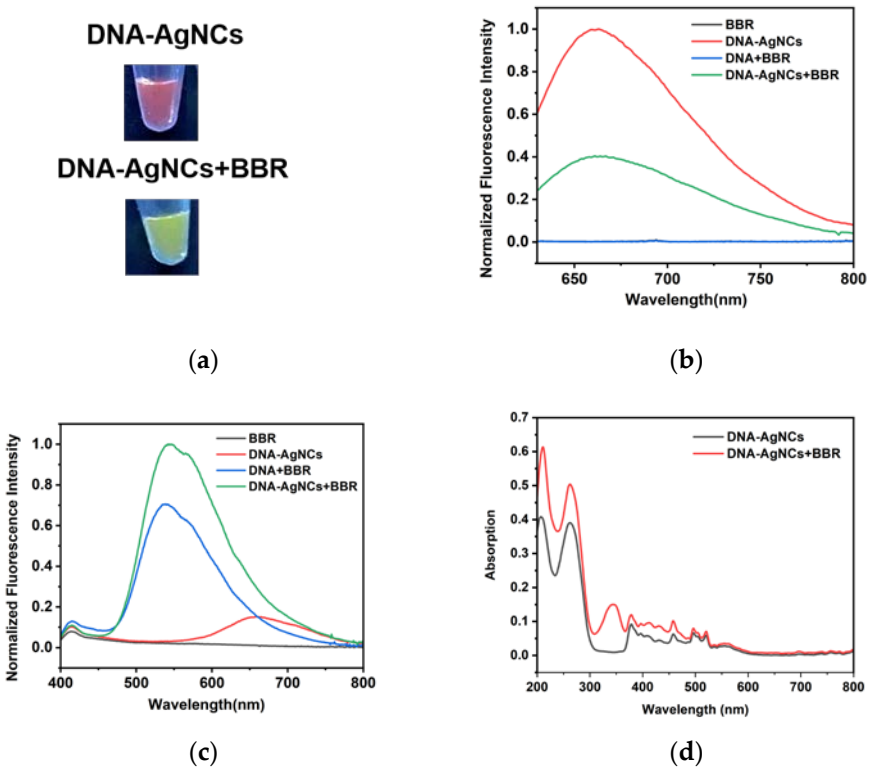

Figure 4. (**a**) The photos of DNA-AgNCs in the absence (up) and presence (down) of BBR under UV light; (**b**) The fluorescence emission spectra of BBR, DNA-AgNCs, DNA+BBR and DNA-AgNCs+BBR excited by 590 nm; (**c**) The fluorescence emission spectra of BBR, DNA-AgNCs, DNA+BBR and DNA-AgNCs+BBR excited by 360 nm. (**d**) The UV-Vis absorption of DNA-AgNCs in the absence (black) and presence (red) of BBR.

Considering the interaction between BBR and triplex was highly dependent on the content of T•A-T (•: Hoogsteen base pairing; -: Watson-Crick base pairing) [8,9], two similar triplex-containing templates with same length but different T•A-T contents (Hp-loop2+ Hp-ss2 and Hp-loop3+Hp-ss3 in Table 1) were designed and utilized for AgNCs synthesis. Comparing with Hp-loop1+Hp-ss1, Hp-loop2+Hp-ss2 had two more T•A-T triplets, while Hp-loop3+Hp-ss3 had two fewer T•A-T triplets. The fluorescence of synthesized DNA-AgNCs and the effect of BBR on DNA-AgNCs fluorescence were shown in Figure 5a and 5b. Comparing with (Hp-loop1+Hp-ss1)-AgNCs, (Hp-loop2+Hp-ss2)-AgNCs exhibited equivalent fluorescence intensity, but less impact on their fluorescence after the addition of BBR. (Hp-loop3+Hp-ss3)-AgNCs had the weakest fluorescence among them. Possible explanation was that cytosine had better affinity to silver ions, and the high content of cytosine in the stem region of Hp-loop3+Hp-ss3 led to less silver ions binding in C6 loop region and resulted in weak fluorescence of synthesized AgNCs. On the other hand, the fluorescence intensity at 560 nm was mainly dependent on the content of T•A-T (Figure 5b) because of the intercalation of BBR in T•A-T triplets. Overall, the ratiometric fluorescence signal was mainly determined by the fluorescence property of DNA-AgNCs among three different templates, and (Hp-loop1+Hp-ss1)-AgNCs were the better probes in BBR detection as a consequence.

 doi:10.20944/preprints202406.1050.v1

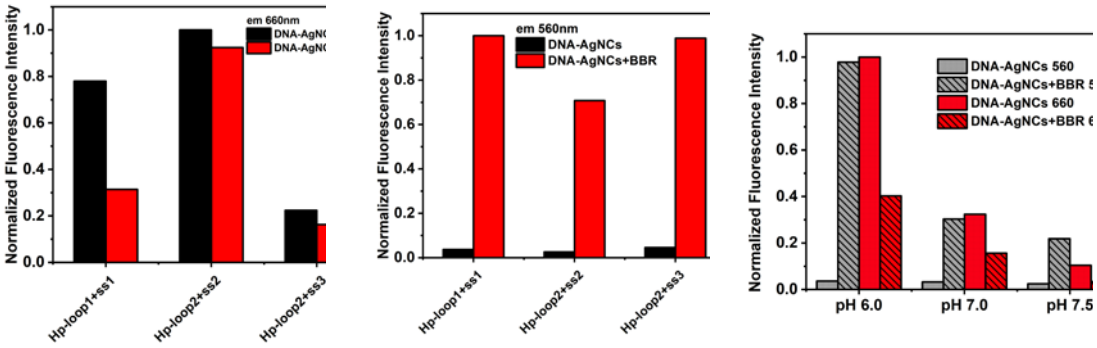

(**a**) (**b**) (**c**)

Figure 5. (**a**) The normalized fluorescence intensity at 660 nm of (Hp-loop1+Hp-ss1)-AgNCs, (Hp-loop2+Hp-ss2)-AgNCs and (Hp-loop3+Hp-ss3)-AgNCs in the absence and presence of BBR; (**b**) The normalized fluorescence intensity at 560 nm of (Hp-loop1+Hp-ss1)-AgNCs, (Hp-loop2+Hp-ss2)-AgNCs and (Hp-loop3+Hp-ss3)-AgNCs in the absence and presence of BBR; (c) The normalized fluorescence intensity of (Hp-loop1+Hp-ss1)-AgNCs at 560 nm and 660 nm in the absence and presence of BBR.

In addition, the best pH condition for BBR interaction was also optimized. The synthesis of DNA-AgNCs and the interaction with BBR were carried out in the buffers at pH 6.0, 7.0 and 7.5, respectively. The results were shown in Figure 5c. Consistent with previous researches, acidic environment was more favorable for the formation of triplex, leading to better fluorescence of both DNA-AgNCs and BBR-triplex complex.

2.3. Detection of BBR

Under the optimal condition, DNA-AgNCs were mixed with different concentration of BBR and incubated for 30 min at room temperature, and the fluorescence intensity at 560 nm and 660 nm were recorded. As shown in Figure 6a and 6b, with the increasing concentration of BBR, the fluorescence at 560 nm enhanced and the fluorescence at 660 nm quenched. The ratiometric fluorescence intensity I_{660}/I_{560} exhibited an excellent linear relationship (I_{660}/I_{560}=-5.60log(C_{BBR})+18.6, R^2=0.997) to the logarithmic values of BBR concentration (Figure 6c). The linear range was from 10 nM to 1000 nM, and the detection limit was 10 nM.

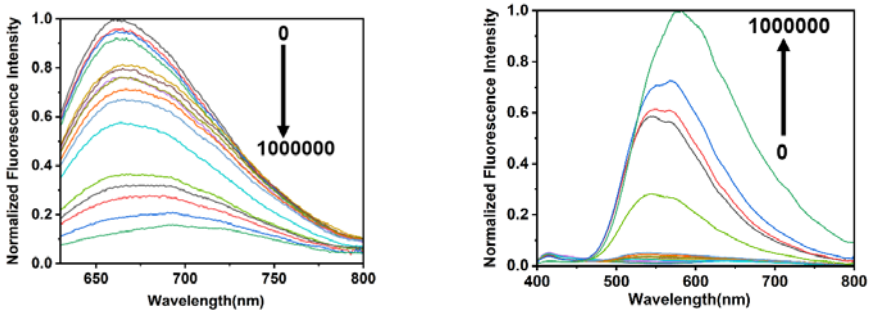

(**a**) (**b**)

 doi:10.20944/preprints202406.1050.v1

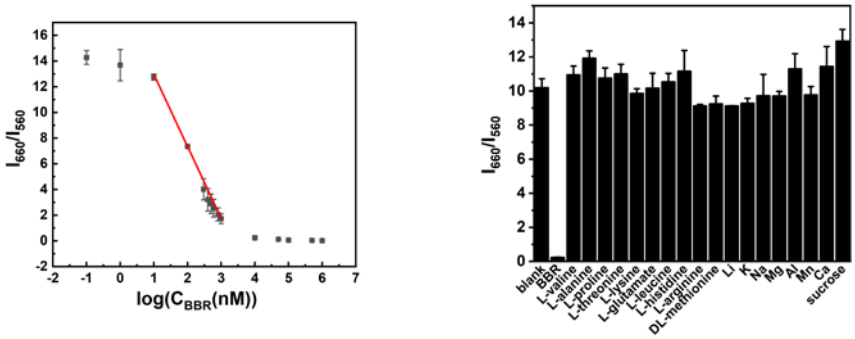

(c) (**d**)

Figure 6. (**a**) The fluorescence spectra of DNA-AgNCs excited by 590 nm in the presence of different concentrations of BBR; (**b**) The fluorescence spectra of DNA-AgNCs excited by 360 nm in the presence of different concentrations of BBR; (**c**) The relationship between ratiometric fluorescence intensity I_{660}/I_{560} and BBR concentration. (**d**) The ratiometric fluorescence intensity I_{660}/I_{560} in the presence of BBR, different amino acids, cations and sucrose at a same concentration.

The selectivity of our sensing method was further investigated. Several common coexisting substances and ions in biological samples were tested for comparison, including L-valine, L-alanine, L-proline, L-threonine, L-histidine, L-glutamic, L-leucine, L-lysine, L–arginine, DL-methionine, Li^+, K^+, Na^+, Mg^{2+}, Zn^{2+}, Al^{3+}, Mn^{2+}, Ca^{2+} and sucrose. Figure 6d showed that all these substances could not cause effective decrease of I_{660}/I_{560}, suggested that our sensing method present an excellent selectivity on BBR.

Our sensing method was further applied in the detection of BBR in real samples. BBR tablets was prepared into solutions with certain concentration and the concentration of BBR was detected by both DNA-AgNCs probes and HPLC. The results were listed in Table 2. The average content of BBR per tablet measured by DNA-AgNCs was 29.80 mg, while the value measured by HPLC was 29.23 mg. These results were close, and both of them were consistent with the labeled amount of 30(±4.5) mg. It demonstrated that our detecting method were able to apply in BBR detection in real samples with a good accuracy.

Table 2. The comparison of BBR contents in BBR tablets detected by our ratiometric fluorescent probes and HPLC.

Method	BBR content (mg)	Average content (mg)	RSD (%)
Ratiometric fluorescence with DNA-AgNCs	29.90	29.80	2.71
	30.64		
	29.02		
HPLC	29.23	29.23	0.07
	29.26		
	2.25		

3. Discussion

DNA-AgNCs are promising fluorescence probes due to their excellent fluorescence property, low cost, easy synthesis, good biocompatibility and low toxicity. Comparing to traditional detection methods, our method does not require complex sample processing or large amount of organic solvents. The fluorescence detection has a short analysis time, and has the potential to finish a large numbers of samples in a short time, improving the analysis efficiency. Especially, as a powerful tool, template DNA can be well designed to achieve better detection results. Normal fluorescence quenching methods often suffer from the interference from the quenching effect of coexisting substances, resulting in false positive results. Ratiometric fluorescence methods greatly improve this problem, enhancing the sensitivity and selectivity and make them resistant to environmental

 doi:10.20944/preprints202406.1050.v1

interference. Therefore, utilizing the interaction between triplex structure and BBR, a triplex-containing DNA-AgNCs were designed to construct novel detecting method of BBR. As a result, a sensitive and selective ratiometric fluorescence method was obtained. The detect limit was 10 nM, which is lower than or equivalent to most fluorescent BBR detection methods.

In addition, the DNA template of our probe presents good biocompatibility, and it is easy to synthesize and modify. Our triplex-containing probe has a short single strand for triplex formation, which can be further modified with different aptamers to improve the targeting ability to specific targets or cells. It suggests great potential in cell imaging and *in vivo* detection. Our probes have been applied in the detection of real samples, and they are expected to apply in pharmacological researches as *in vivo* probes in the future, providing new ideas for mechanism studies and new drug development.

4. Materials and Methods

4.1. Oligodeoxynucleotides and Materials

All DNA sequences in this work were purchased from Shanghai Sangon Biotechnology Co. Ltd. (Shanghai, China) and used without further purification. The sequences were listed in Table 1. DNA samples were dissolved in distilled water purified by Thermo Type 2 system (Germany), and stored in -20°C before use. Silver nitrate and sodium borohydride purchased from Sigma-Aldrich. Other reagents were obtained from Shanghai Yuanye Biotechnology Co., Ltd. All solution were prepared in distilled water purified by a Thermo Type 2 system (Thermo, Langenselbold, Germany).

4.2. Synthesis of DNA-AgNCs

10 μM of template DNA in sodium phosphate buffer (PB, 0.2 M, pH=6.0) was incubated at 90 °C for 5 min and then cooled from 90 °C to room temperature. The DNA sample mixed with 60 μM of $AgNO_3$ and incubated at room temperature for 10 min. 60 μM of fresh $NaBH_4$ was later added with vigorous shaking for 10 min. The solution was kept in the dark at 4 °C for 24 h before fluorescence characterization.

4.3. Characterization of DNA-AgNCs

The UV-Visible spectra of DNA-AgNCs were recorded by Aurora-900 ultramicro spectrophotometer(Hangzhou Haipei Instrument Co., Ltd, China). The size of DNA-AgNCs were characterized by a H-600 transmission electron microscope (Hitachi, Ltd., Japan). Circular dichroism (CD) spectra were collected by a JASCO J-820 spectropolarimeter (JASCO Corporation, Japan).

4.4. Fluorescence Measurement

Fluorescence of DNA-AgNCs were performed with a SpectraMax Paradigm Multi-Mode Detection Platform system (Molecular Devices, USA) with a final concentration of 1 μM. For BBR detection, the prepared DNA-AgNCs solutions were mixed with different concentrations of BBR, and the fluorescence were conducted after 0.5 h incubation.

4.4. Real Sample Detection

The DNA-AgNCs were applied in the detection of BBR in Compound Berberine Tablets (BBR tablets, Hubei Nordsheng Pharmaceutical Co., Ltd). Fifteen BBR tablets were crushed and ground, weighed, and divided into three parts of powder on average. The three parts of powder were respectively dissolved and filtered into a solution of proper concentration. The accurate concentration of BBR solution was further determined by fluroescence with DNA-AgNCs and high-performance liquid chromatography (HPLC, Agilent 1260), respectively. For HPLC detection, the chromatographic column was a ZORBAX SB-C18 column (4.6 mm × 250 mm, 5 μm). The separation was performed by isocratic elution at a flow rate of 1.0 mL/min at 30 °C, using a mobile phase of 25:75

 doi:10.20944/preprints202406.1050.v1

acetonitrile and KH_2PO_4 (0.01M). The injection volume was 10 μL, and the detection wavelength was 265 nm.

5. Conclusions

In conclusion, a simple, sensitive and selective fluorescence detecting method of BBR was constructed with triplex-containing DNA-AgNCs. Utilizing the specific interaction between triplex structure and BBR, the red fluorescence of DNA-AgNCs was quenched and the complex of triplex-BBR emitted yellow green fluorescence. The ratiometric fluorescence intensity exhibited a linear relationship with BBR concentration in a range from 10 to 1000 nM, with a limit of detection of 10 nM. This method has been used in real sample detection, and it is promising for in vivo analysis due to the easy modification and strong specificity of DNA.

Supplementary Materials: The following supporting information can be downloaded at: www.mdpi.com/xxx/s1, Figure S1: title; Table S1: title; Video S1: title.

Author Contributions: Conceptualization, M.Z. and Y.T.; methodology, M.Z., M.S. and J.L.; validation, M.Z., M.S. and J.L.; formal analysis, Y.T.; investigation, M.Z., M.S. and J.L.; resources, C.C., Y.Y. and Y.T.; data curation, M.Z. and Y.T.; writing—original draft preparation, M.Z. and Y.T.; writing—review and editing, Y.Y. and Y.T. ; visualization, M.Z. and Y.T.; supervision, C.C., Y.Y. and Y.T.; project administration, Y.Y. and Y.T.; funding acquisition, Y.Y. and Y.T. All authors have read and agreed to the published version of the manuscript.

Funding: This research was funded by National Natural Science Foundation of China, grant number 82204650, and Jilin Province Science and Technology Development Plan Item, grant number 20210401055YY.

Data Availability Statement: The original contributions presented in the study are included in the article/supplementary material, further inquiries can be directed to the corresponding authors.

Conflicts of Interest: The authors declare no conflicts of interest.

References

1. Cicero, A.F.G.; Baggioni, A. Berberine and Its Role in Chronic Disease. Adv Exp Med Biol 2016, 928, 27-45, doi:10.1007/978-3-319-41334-1_2.
2. Jin, Y.; Khadka, D.B.; Cho, W.-J. Pharmacological effects of berberine and its derivatives: a patent update. Expert Opin. Ther. Pat. 2015, 26, 229-243, doi:10.1517/13543776.2016.1118060.
3. Liu, Z.; Wang, X.; Zhang, H.; Zhang, S.; Li, Y.; Liu, Y.; Peng, D. Synthesis and anti-inflammatory effects of a series of novel 9-O-substituted berberine derivatives. Med. Chem. Res. 2017, 26, 672-679, doi:10.1007/s00044-017-1787-z.
4. Liu, X.; Yu, M.; Liang, J. Research Progress on the Synthesis of Protoberberine Skeleton and Its Anti-inflammatory Activity. Chinese Journal of Organic Chemistry 2023, 43, 1325-1340, doi:10.6023/cjoc202209037.
5. Zhang, L.C.; Wu, X.Y.; Yang, R.B.; Chen, F.; Liao, Y.; Zhu, Z.F.; Wu, Z.D.; Sun, X.; Wang, L.F. Effects of Berberine on the Gastrointestinal Microbiota. Front Cell Infect Mi 2021, 10, doi:10.3389/fcimb.2020.588517.
6. Chuang, T.C.; Wu, K.H.; Lin, Y.Y.; Kuo, H.P.; Kao, M.C.; Wang, V.; Hsu, S.C.; Lee, S.L. Dual down-regulation of EGFR and ErbB2 by berberine contributes to suppression of migration and invasion of human ovarian cancer cells. Environ. Toxicol. 2021, 36, 737-747, doi:10.1002/tox.23076.
7. Debnath, D.; Kumar, G.S.; Maiti, M. Circular Dichroism Studies of the Structure of DNA Complex with Berberine. Journal of Biomolecular Structure and Dynamics 1991, 9, 61-79, doi:10.1080/07391102.1991.10507893.
8. Das, S.; Kumar, G.S.; Ray, A.; Maiti, M. Spectroscopic and thermodynamic studies on the binding of sanguinarine and berberine to triple and double helical DNA and RNA structures. J. Biomol. Struct. Dyn. 2003, 20, 703-713, doi:Doi 10.1080/07391102.2003.10506887.
9. Keppler, M.D.; Neidle, S.; Fox, K.R. Stabilisation of TG- and AG-containing antiparallel DNA triplexes by triplex-binding ligands. Nucleic acids research 2001, 29, 1935-1942, doi:10.1093/nar/29.9.1935.
10. Oliva, R.; Mukherjee, S.; Manisegaran, M.; Campanile, M.; Del Vecchio, P.; Petraccone, L.; Winter, R. Binding Properties of RNA Quadruplex of SARS-CoV-2 to Berberine Compared to Telomeric DNA Quadruplex. Int J Mol Sci 2022, 23, doi:10.3390/ijms23105690.
11. Xu, L.; Hong, S.; Sun, N.; Wang, K.; Zhou, L.; Ji, L.; Pei, R. Berberine as a novel light-up i-motif fluorescence ligand and its application in designing molecular logic systems. Chem. Commun. 2016, 52, 179-182, doi:10.1039/c5cc08242k.

 doi:10.20944/preprints202406.1050.v1

12. Hu, Z.; Xie, M.; Yang, D.; Chen, D.; Jian, J.; Li, H.; Yuan, K.; Jiang, Z.; Zhou, H. A simple, fast, and sensitive colorimetric assay for visual detection of berberine in human plasma by NaHSO₄-optimized gold nanoparticles. Rsc Adv. 2017, 7, 34746-34754, doi:10.1039/c7ra05291j.
13. Song, Z.; Zhao, T.; Wang, L.; Xiao, Z. Chemiluminescence flow sensor for berberine with immobilized reagents. Bioorg. Med. Chem. 2001, 9, 1701-1705, doi:10.1016/s0968-0896(01)00069-4.
14. Wen, A.; Peng, X.; Zhang, P.; Long, Y.; Gong, H.; Xie, Q.; Yue, M.; Chen, S. Spectrofluorometric determination of berberine using a novel Au nanocluster with large Stokes shift. Analytical and Bioanalytical Chemistry 2018, 410, 6489-6495, doi:10.1007/s00216-018-1246-9.
15. Xiong, J.; Yang, L.; Gao, L.X.; Zhu, P.P.; Chen, Q.; Tan, K.J. A highly fluorescent lanthanide metal-organic framework as dual-mode visual sensor for berberine hydrochloride and tetracycline. Analytical and Bioanalytical Chemistry 2019, 411, 5963-5973, doi:10.1007/s00216-019-02004-9.
16. Wang, J.-S.; Sakthivel, R.; Anbazhagan, R.; krishnamoorthi, R.; Kubendhiran, S.; Lai, J.-Y.; Tsai, H.-C.; Chen, S.-M. Electroactive polypyrrole-molybdenum disulfide nanocomposite for ultrasensitive detection of berberine in rat plasma. Analytica Chimica Acta 2020, 1125, 210-219, doi:10.1016/j.aca.2020.05.056.
17. Wu, T.-Y.; Chang, F.-R.; Liou, J.-R.; Lo, I.W.; Chung, T.-C.; Lee, L.-Y.; Chi, C.-C.; Du, Y.-C.; Wong, M.-H.; Juo, S.-H.H.; et al. Rapid HPLC Quantification Approach for Detection of Active Constituents in Modern Combinatorial Formula, San-Huang-Xie-Xin-Tang (SHXXT). Front. Pharmacol. 2016, 7, doi:10.3389/fphar.2016.00374.
18. Yuan, Z.-W.; Leung, E.L.-H.; Fan, X.-X.; Zhou, H.; Ma, W.-Z.; Liu, L.; Xie, Y. Quantitative evaluation of berberine subcellular distribution and cellular accumulation in non-small cell lung cancer cells by UPLC-MS/MS. Talanta 2015, 144, 20-28, doi:10.1016/j.talanta.2015.05.017.
19. Liu, S.P.; Yang, Z.; Liu, Z.F.; Liu, J.T.; Shi, Y. Resonance Rayleigh scattering study on the interaction of gold nanoparticles with berberine hydrochloride and its analytical application. Analytica Chimica Acta 2006, 572, 283-289, doi:10.1016/j.aca.2006.05.058.
20. Lu, Y.; Chen, W. Sub-nanometre sized metal clusters: from synthetic challenges to the unique property discoveries. Chem Soc Rev 2012, 41, 3594-3623, doi:10.1039/c2cs15325d.
21. Shang, L.; Dong, S.; Nienhaus, G.U. Ultra-small fluorescent metal nanoclusters: Synthesis and biological applications. Nano Today 2011, 6, 401-418, doi:10.1016/j.nantod.2011.06.004.
22. Diez, I.; Ras, R.H.A. Fluorescent silver nanoclusters. Nanoscale 2011, 3, 1963-1970, doi:10.1039/c1nr00006c.
23. Richards, C.I.; Choi, S.; Hsiang, J.C.; Antoku, Y.; Vosch, T.; Bongiorno, A.; Tzeng, Y.L.; Dickson, R.M. Oligonucleotide-stabilized Ag nanocluster fluorophores. Journal of the American Chemical Society 2008, 130, 5038-+, doi:10.1021/ja8005644.
24. Zhou, B.; Khan, I.M.; Ding, X.; Niazi, S.; Zhang, Y.; Wang, Z. Fluorescent DNA-Silver nanoclusters in food safety detection: From synthesis to application. Talanta 2024, 273, doi:10.1016/j.talanta.2024.125834.
25. Pandya, A.; Lad, A.N.; Singh, S.P.; Shanker, R. DNA assembled metal nanoclusters: synthesis to novel applications. Rsc Adv. 2016, 6, 113095-113114, doi:10.1039/C6RA24098D.
26. Guo, W.; Yuan, J.; Dong, Q.; Wang, E. Highly Sequence-Dependent Formation of Fluorescent Silver Nanoclusters in Hybridized DNA Duplexes for Single Nucleotide Mutation Identification. Journal of the American Chemical Society 2010, 132, 932-+, doi:10.1021/ja907075s.